

# Ca<sup>2+</sup> Oscillations Promote APC/C-Dependent Cyclin B1 Degradation during Metaphase Arrest and Completion of Meiosis in Fertilizing Mouse Eggs

Victoria L. Nixon, Mark Levasseur,  
Alex McDougall, and Keith T. Jones<sup>1</sup>  
Department of Physiological Sciences  
The Medical School  
Framlington Place  
University of Newcastle  
Newcastle, NE2 4HH  
United Kingdom

## Summary

Cyclin B1, the regulatory component of M phase-promoting factor (MPF), is degraded during the metaphase-anaphase transition in an anaphase-promoting complex/cyclosome (APC/C)-dependent process [1]. MPF activity is stable in eggs, and a sperm-triggered Ca<sup>2+</sup> signal is needed to promote cyclin degradation [2]. In frogs, a single Ca<sup>2+</sup> spike promotes cell cycle resumption, but, in mammals, the Ca<sup>2+</sup> signal is more complex, consisting of a series of spikes that stop several hours after sperm fusion [3]. Using dual imaging in mouse eggs, we have examined how the Ca<sup>2+</sup> signal generates cyclin B1 destruction using destructible and nondestructible GFP-tagged constructs. APC/C activity was present in unfertilized eggs, giving cyclin B1 a half-life of  $1.15 \pm 0.28$  hr. However, APC/C-dependent cyclin degradation was elevated 6-fold when sperm raised cytosolic Ca<sup>2+</sup> levels above 600 nM. This activation was transitory since cyclin B1 levels recovered between Ca<sup>2+</sup> spikes. For continued cyclin degradation at basal Ca<sup>2+</sup> levels, multiple spikes were needed. APC/C-mediated degradation was observed until eggs had completed meiosis with the formation of pronuclei, and, at this time, Ca<sup>2+</sup> spikes stopped. Therefore, the physiological need for a repetitive Ca<sup>2+</sup> signal in mammals is to ensure long-term cyclin destruction during a protracted exit from meiosis.

## Results and Discussion

Fertilization in most species generates a rise in cytosolic Ca<sup>2+</sup> that is both necessary and sufficient to cause cell cycle resumption following metaphase arrest [4]. Ca<sup>2+</sup> acts to decrease MPF activity, which is high at metaphase, and also cytotstatic factor (CSF), which is responsible for MPF stabilization before egg activation [2, 5–8]. In frogs, from which most is known, a single Ca<sup>2+</sup> wave initiated by the sperm acts through calmodulin-dependent protein kinase II (CaMKII) to activate APC/C ubiquitin ligase activity, thereby targeting cyclin B1 for proteolysis [5–6]. Thus, loss of MPF and entry into the first embryonic cell cycle is achieved within 10 min.

Less is known of the dynamics of cyclin B1 destruction in mammalian eggs, in which some aspects of meiosis are different than those of frog. In mammals, meiotic

exit lasts hours rather than minutes, and fertilization is associated with a characteristic series of Ca<sup>2+</sup> spikes rather than a single Ca<sup>2+</sup> rise [4]. Indeed, a single Ca<sup>2+</sup> rise is generally regarded as a poor stimulus for parthenogenesis in mammalian eggs [9]. Therefore, we wanted to examine cyclin B1 turnover in real time in individual mouse eggs and determine its dynamics following the sperm-triggered Ca<sup>2+</sup> signals. In order to achieve this, we employed two enhanced green fluorescent protein (eGFP) constructs (Figure 1A): full-length cyclin B1 (cyclin B1::GFP) and a truncated cyclin B1 lacking its N-terminal 90 amino acids ( $\Delta 90$  cyclin B1::GFP).  $\Delta 90$  cyclin B1::GFP is not a substrate for polyubiquitination by the APC/C since it lacks its destruction box [10, 11].

## APC/C-Dependent Cyclin B1 Degradation in Metaphase-Arrested Eggs

Using the aforementioned cyclin constructs, we found that unfertilized eggs had an active APC/C. The destruction box of cyclin B1 is portable in sea urchins, yeast, and mammalian cells [11–13], so that association with CDK1 is not essential for ubiquitin-mediated proteolysis. Therefore, cyclin B1::GFP is used here as a marker for APC/C-dependent proteolysis, rather than as a marker for MPF activity. To determine APC/C-mediated destruction of cyclin B1, the drop in GFP fluorescence was followed after synthesis of exogenously added cyclin B1::GFP was blocked. To confer some degree of specificity in synthesis inhibition, antisense deoxyribonucleotide to GFP was used in preference to cycloheximide. Antisense deoxynucleotide to GFP when microinjected into eggs blocked cyclin B1::GFP synthesis and led to an exponential decay in cyclin B1::GFP fluorescence (Figure 1B), with a half-time for cyclin destruction of  $1.15 \pm 0.28$  hr (mean  $\pm$  SD). This degradation was APC/C dependent, since the same experiments performed with  $\Delta 90$  cyclin B1::GFP showed no destruction. Consistent with a block in degradation, through N terminus deletion of the destruction box and a block in translation by the introduction of antisense deoxynucleotide,  $\Delta 90$  cyclin B1::GFP fluorescence levels stayed constant after antisense microinjection (Figure 1B).

The presence of an active APC/C in metaphase II-arrested mouse eggs could also be observed by using a microtubule-disrupting agent, which prevents APC/C activation by the induction of a spindle checkpoint [14]. Incubation of cyclin B1::GFP-mRNA-injected eggs with colcemid led to a faster reported rate of cyclin B1 production and, consequently, greater levels of cyclin B1 protein (Figure 1B). Note that the total fluorescence levels achieved with cyclin B1::GFP in the presence of colcemid exceeded those of  $\Delta 90$  cyclin B1::GFP, despite the fact that both constructs are protected from APC/C-dependent destruction. However, this is likely to reflect inherent differences in translation rates between mRNAs, as noted previously for truncated cyclin B1 constructs compared to full-length cyclin B1 [15].

<sup>1</sup>Correspondence: k.t.jones@ncl.ac.uk

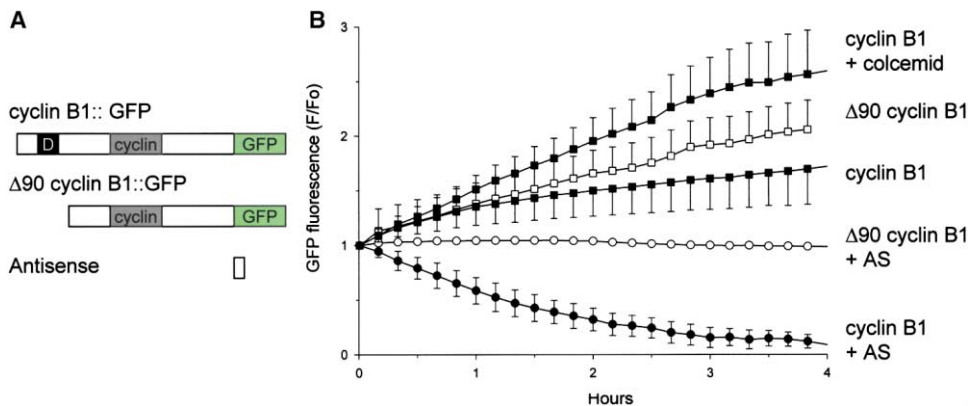


Figure 1. Rapid APC/C-Dependent Cyclin B1 Degradation in Unfertilized Mouse Eggs

(A) Constructs used in the present study. Full-length human cyclin B1 and  $\Delta 90$  cyclin B1 mRNA constructs were made by tagging with eGFP [29]. Cyclin: conserved cyclin box necessary for CDK binding, D: destruction box. An antisense (AS) phosphothiorate-linked deoxyribonucleic acid construct (5'-GAAAAGTTCTTCTCTTACT-3') was designed against the N terminus of eGFP (MWG-Biotech).

(B) Eggs were microinjected as described [30, 31] with 0.5 mg/ml mRNA of cyclin B1::GFP (closed symbols,  $n = 43$ ) or  $\Delta 90$  cyclin B1::GFP (open symbols,  $n = 23$ ). Some eggs were further microinjected with 0.5 mg/ml AS (circles;  $n = 9$ , full-length cyclin B1;  $n = 6$ ,  $\Delta 90$  cyclin B1) or were incubated in 100 ng/ml colcemid-containing medium ( $n = 19$ ). Cyclin B1 levels are recorded as a ratio of fluorescence at time  $t$  ( $F$ ) and time 0 hr ( $F_0$ ). Datapoints represent means, and error bars represent standard deviations. Note that the error bars for experiments involving  $\Delta 90$  cyclin B1::GFP in the presence of the antisense construct are smaller than the symbols used to plot the mean and so are not shown on the figure.

#### Rapid but Transitory Cyclin B1 Destruction Caused by the First Sperm-Induced $\text{Ca}^{2+}$ Spike

To establish the relationship between cyclin B1 destruction and the long-lasting  $\text{Ca}^{2+}$  signal that is unique to mammals, mouse eggs were imaged simultaneously for  $\text{Ca}^{2+}$  and GFP by microinjection of the  $\text{Ca}^{2+}$  fluoro-chrome fura2-dextran and mRNA of full-length cyclin B1::GFP. Following insemination, we observed a transitory period of cyclin B1 destruction that was short in duration and coincident with the initial sperm-triggered  $\text{Ca}^{2+}$  rise (Figure 2A). From the rates of cyclin B1 destruction and synthesis plotted in Figure 1B, it was calculated that, during the first  $\text{Ca}^{2+}$  spike, there was a  $6.3 \pm 0.7$  (mean  $\pm$  SEM)-fold increase in cyclin B1 destruction. The onset of cyclin B1 destruction showed no obvious lag in relation to the cytosolic  $\text{Ca}^{2+}$  rise but was instead associated with the exponential rising phase of the  $\text{Ca}^{2+}$  spike.

We needed to perform control experiments in order to show that the drop in GFP fluorescence associated with the  $\text{Ca}^{2+}$  rise was not an imaging artifact. Ubiquitination by itself, in the absence of proteasomal activity, does not quench fluorescence of the construct but, as predicted, stabilizes it [16]. However, the drop in the GFP signal seen here could have been due to a spillover in the fura2 signal or a form of fluorescence resonance energy transfer. This was not the case, since no drop in GFP levels was observed during the first sperm-induced  $\text{Ca}^{2+}$  spike when eggs expressing cyclin B1::GFP were inseminated in the presence of colcemid to inhibit APC/C activity ( $n = 22$ , data not shown). Furthermore, no change in GFP fluorescence was observed if eggs were expressing  $\Delta 90$  cyclin B1::GFP ( $n = 23$ ; Figure 2B). Therefore, we conclude that the recorded changes in GFP fluorescence were not an imaging artifact but instead were a result of  $\text{Ca}^{2+}$ -promoted cyclin B1 destruction through the APC/C.

In both frog [5, 6] and mouse [17] eggs, the immediate target for  $\text{Ca}^{2+}$  action is CaMKII, but at which point CaMKII feeds into the cyclin B1 destruction pathway is not known. The instantaneous increase in cyclin B1 destruction occurring with the first  $\text{Ca}^{2+}$  spike suggests  $\text{Ca}^{2+}$  action downstream in the cyclin destruction pathway, maybe on the proteasome itself. Indeed, the ability of  $\text{Ca}^{2+}$  to promote the 26S proteasome has been characterized both in *Xenopus* [18] and ascidian [19] eggs. However, at least in frog, where it has been calculated, the half-life of ubiquitinated cyclin B1 is 90 s [11], and millimolar  $\text{Ca}^{2+}$  levels in *in vitro* studies can enhance polyubiquitination of p53 [20]. Therefore, the present data do not rule out direct promotion of APC/C activity.

#### Incremental Cyclin B1 Degradation Caused by a Series of $\text{Ca}^{2+}$ Spikes

In the immediate period following the first sperm-triggered  $\text{Ca}^{2+}$  rise, the net rate of cyclin B1 synthesis was not different statistically from the rate preceding any  $\text{Ca}^{2+}$  change (Figures 2A and 3A). In order to observe a sustained net destruction of cyclin B1, we needed to look at additional sperm-triggered  $\text{Ca}^{2+}$  spikes. In eggs in which the magnitudes of the subsequent  $\text{Ca}^{2+}$  spikes were as large as the initial rise, discrete drops in cyclin B1 levels continued to be associated with each  $\text{Ca}^{2+}$  spike (Figure 3A). This was not so in inseminated eggs in which  $\text{Ca}^{2+}$  spikes were of a smaller magnitude (Figure 3B). The critical  $\text{Ca}^{2+}$  concentration needed to trigger immediate cyclin B1 destruction was 600 nM (Figure 3C). However, independent of the magnitude of the spikes, a progressive fall in cyclin B1 levels occurred, which was not confined to periods of raised cytosolic  $\text{Ca}^{2+}$  (Figures 3A and 3B).

The CaM-trapping ability of CaMKII results in it remaining active between  $\text{Ca}^{2+}$  spikes, and therefore it can potentially decode a frequency-encoded signal. Such

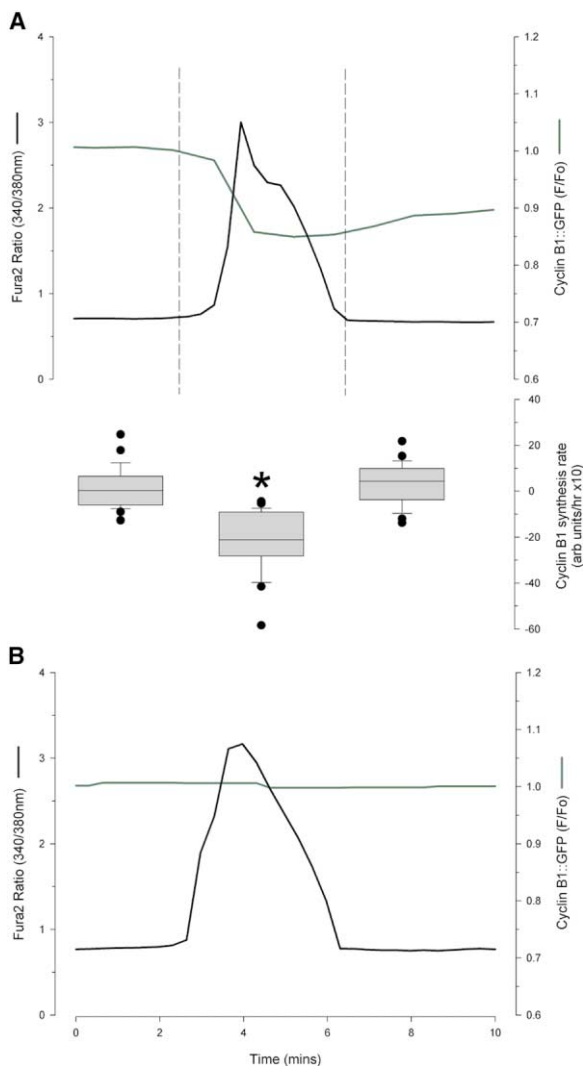


**Figure 2. Immediate APC/C-Dependent Cyclin B1 Destruction Associated with the First Sperm-Triggered  $\text{Ca}^{2+}$  Spike**

(A) Inseminated eggs coinjected with fura2-dextran and mRNA of full-length cyclin B1::GFP [30, 31]. The vertical dashed lines represent the start and end of the first sperm-induced  $\text{Ca}^{2+}$  spike. Net changes in cyclin B1::GFP levels were calculated for the periods preceding, during, and following the  $\text{Ca}^{2+}$  rise and were plotted as a box-and-whisker plot [32]. The median and 25th and 75th percentile form the box, while the 10th and 90th percentiles are the error bars; data points outside this range are plotted individually. An asterisk indicates that the group is significantly different from other groups; paired t test,  $p < 0.0001$  ( $n = 24$ ).

(B) As in (A), but in eggs expressing  $\Delta 90$  cyclin B1 ( $n = 23$ ).

highly nonlinear behavior of CaMKII has been predicted by in silico modeling and by superfusion experiments in vitro [21, 22]. The simplest interpretation of our data is that we are observing the same phenomenon of CaMKII activation intracellularly. These present data also help explain the apparent paradox that, although inositol 1,4,5-trisphosphate ( $\text{InsP}_3$ ) is clearly the second messenger responsible for  $\text{Ca}^{2+}$  spikes at fertilization [23], some lower concentrations of  $\text{InsP}_3$  that release  $\text{Ca}^{2+}$  and generate  $\text{Ca}^{2+}$  spikes do not activate eggs [24]. This is because the trapping ability of CaMKII for CaM is

dependent on both the amplitude and the frequency of the  $\text{Ca}^{2+}$  spikes, such that a series of small amplitude  $\text{Ca}^{2+}$  spikes would not be sufficient to promote CaM trapping.

### Cyclin B1 Degradation Stops When Meiosis Is Complete

We observed  $\text{Ca}^{2+}$ -promoted cyclin B1 destruction in eggs throughout the period of meiotic exit, until the very last  $\text{Ca}^{2+}$  spike (Figure 4). In our experiments [3] and those of others [25], pronuclei are usually visible once the  $\text{Ca}^{2+}$  oscillations have stopped. Following pronuclei formation, the net rate of cyclin B1 synthesis was  $3.4 \pm 1.6$  (mean  $\pm$  SD,  $n = 20$ ) times faster than before fertilization, at metaphase II. In mouse, S phase begins about 8 hr after fertilization, around the time that nucleoli form in pronuclei [26]. Therefore, the experiments here show that APC/C activity is switched off at S phase, a finding that would be consistent with the known cell cycle regulation of APC/C activity [27, 28].

In summary, we have used a GFP-based approach to examine real-time cyclin destruction in mouse eggs. In mitotic cells, cyclin B1 destruction is associated with chromosome alignment at metaphase [16]. In mouse eggs, whose sister chromatids are already aligned at metaphase before fertilization, we found that the APC/C is active, resulting in a short half-life for cyclin B1 of about 1 hr. However, sperm induced an immediate 6-fold increase in APC/C-mediated cyclin B1 destruction when it raised intracellular  $\text{Ca}^{2+}$  levels above 600 nM. This effect was transitory, and repetitive  $\text{Ca}^{2+}$  spikes were required to initiate continuous cyclin B1 destruction during meiotic exit until entry into S phase. Direct visualization of cyclin B1 turnover in fertilized mouse eggs has therefore demonstrated the physiological basis for repetitive  $\text{Ca}^{2+}$  spikes, which have been previously reported in a number of mammalian eggs. They ensure continuous cyclin B1 destruction during a protracted exit from meiosis.

### Supplementary Material

Supplementary Material including the Experimental Procedures, and, as a further control experiment, a trace of GFP::cyclin B1 levels in an inseminated egg not microinjected with fura2-dextran is available at <http://images.cellpress.com/supmat/supmatin.htm>.

### Acknowledgments

The Wellcome Trust funded this work as a project grant to K.T.J.

Received: February 15, 2002

Revised: March 12, 2002

Accepted: March 12, 2002

Published: April 30, 2002

### References

1. Morgan, D.O. (1999). Regulation of the APC and the exit from mitosis. *Nat. Cell Biol.* 1, E47–E53.
2. Kubiak, J.Z., Weber, M., de Pennart, H., Winston, N.J., and Maro, B. (1993). The metaphase II arrest in mouse oocytes is controlled through microtubule-dependent destruction of cyclin B in the presence of CSF. *EMBO J.* 12, 3773–3778.
3. Jones, K.T., Carroll, J., Merriman, J.A., Whittingham, D.G., and Kono, T. (1995). Repetitive sperm-induced  $\text{Ca}^{2+}$  transients in

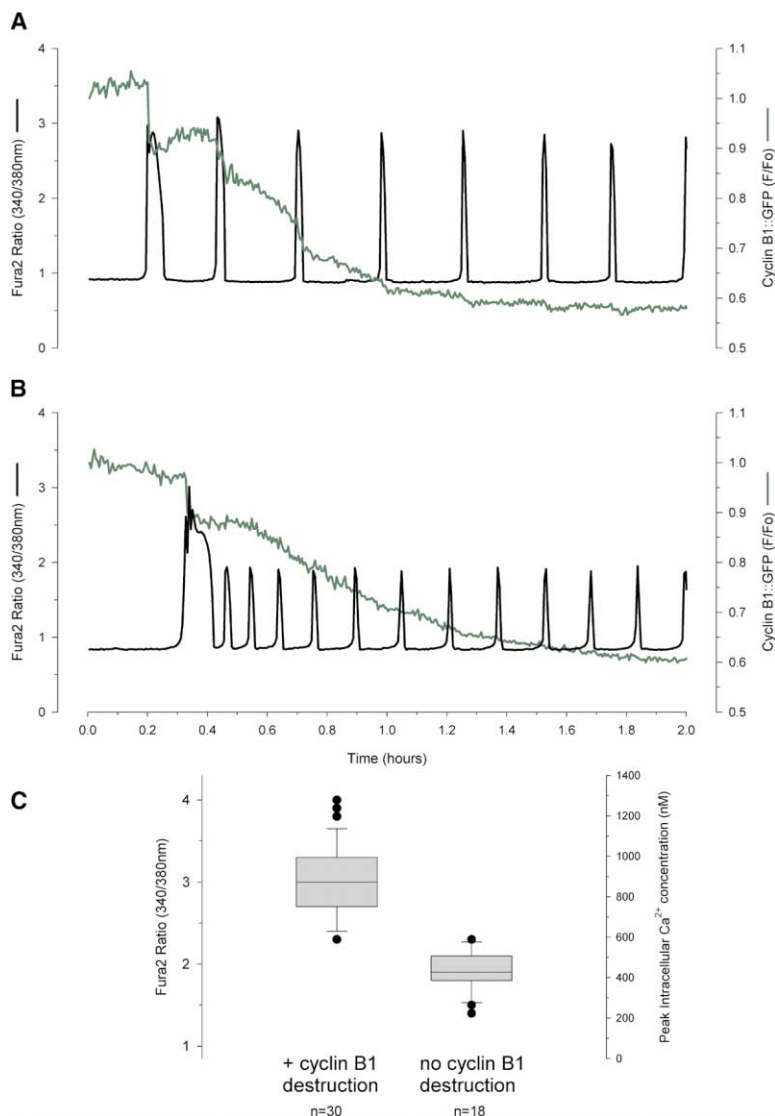


**Figure 3.  $\text{Ca}^{2+}$ -Promoted Cyclin B1 Destruction during the Period of Long-Lasting  $\text{Ca}^{2+}$  Spikes**

(A and B) Insemination of eggs expressing full-length cyclin B1::GFP.

(C) Intracellular  $\text{Ca}^{2+}$  was calibrated [3], and the magnitudes of the first two  $\text{Ca}^{2+}$  spikes in inseminated eggs were calculated. They were chosen because, in any one egg, the first two spikes show the greatest difference in amplitude [33]. The spikes were grouped into those that had been associated with an immediate drop in cyclin B1 levels and those that were not. The amplitude of the spike was then plotted for both groups in a box-and-whisker format.

- mouse oocytes are cell cycle dependent. *Development* 121, 3259–3266.
- Stricker, S.A. (1999). Comparative biology of calcium signalling during fertilization and egg activation in animals. *Dev. Biol.* 211, 157–176.
  - Lorca, T., Galas, S., Fesquet, D., Devault, A., Cavadore, J., and Doree, M. (1991). Degradation of the proto-oncogene product p39<sup>mos</sup> is not necessary for cyclin proteolysis and exit from meiotic metaphase: requirement for a  $\text{Ca}^{2+}$ -calmodulin dependent event. *EMBO J.* 10, 2087–2093.
  - Lorca, T., Cruzalegui, F.H., Fesquet, D., Cavadore, J., Mery, J., Means, A., and Doree, M. (1993). Calmodulin-dependent protein kinase II mediates inactivation of MPF and CSF upon fertilization of *Xenopus* eggs. *Nature* 366, 270–273.
  - Weber, M., Kubiak, J.Z., Arlinghaus, R.B., Pines, J., and Maro, B. (1991). C-mos proto-oncogene product is partly degraded after release from meiotic arrest and persists during interphase in mouse zygotes. *Dev. Biol.* 148, 393–397.
  - Zernicka-Goetz, M., Ciernerych, M.A., Kubiak, J.Z., Tarkowski, A.K., and Maro, B. (1995). Cytostatic factor inactivation is induced by a calcium-dependent mechanism present until the second cell cycle in fertilized but not in parthenogenetically activated mouse eggs. *J. Cell Sci.* 108, 469–474.
  - Whittingham, D.G. (1980). Parthenogenesis in mammals. In *Oxford Reviews in Reproductive Biology*, C. Finn, ed. (Oxford: Oxford University Press), pp. 205–231.

- Hershko, A., Ganoth, D., Pehrson, J., Palazzo, R.E., and Cohen, L.H. (1991). Methylated ubiquitin inhibits cyclin degradation in clam embryo extracts. *J. Biol. Chem.* 266, 16376–16379.
- Glotzer, M., Murray, A.W., and Kirschner, M.W. (1991). Cyclin is degraded by the ubiquitin pathway. *Nature* 349, 132–138.
- Brandeis, M., and Hunt, T. (1996). The proteolysis of mitotic cyclins in mammalian cells persists from the end of mitosis until the onset of S phase. *EMBO J.* 15, 5280–5289.
- Amon, A., Imniger, S., and Nasmyth, K. (1994). Closing the cell cycle circle in yeast: G2 cyclin proteolysis initiated at mitosis persists until the activation of G1 cyclins in the next cell cycle. *Cell* 77, 1037–1050.
- Gorbsky, G.J. (1997). Cell cycle checkpoints: arresting progress in mitosis. *Bioessays* 19, 193–197.
- Murray, A.W., Solomon, M.J., and Kirschner, M.W. (1989). The role of cyclin synthesis and degradation in the control of maturation promoting factor activity. *Nature* 339, 280–286.
- Clute, P., and Pines, J. (1999). Temporal and spatial control of cyclin B1 destruction in metaphase. *Nat. Cell Biol.* 1, 82–87.
- Winston, N.J., and Maro, B. (1995). Calmodulin-dependent protein kinase II is activated transiently in ethanol-stimulated mouse oocytes. *Dev. Biol.* 170, 350–352.
- Aizawa, H., Kawahara, H., Tanaka, K., and Yokosawa, H. (1996). Activation of the proteasome during *Xenopus* egg activation implies a link between proteasome activation and intracellular calcium release. *Biochem. Biophys. Res. Comm.* 218, 224–228.

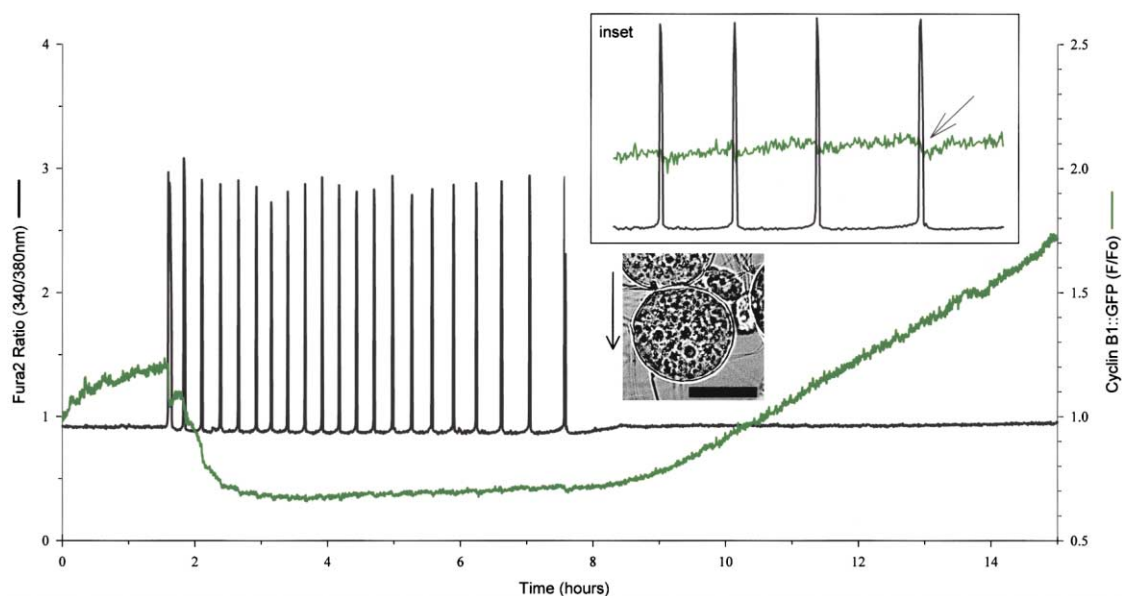


Figure 4. Cyclin B1 Destruction Continues until Meiosis Is Complete.

Cyclin B1::GFP levels increased in inseminated eggs when the  $\text{Ca}^{2+}$  spikes stopped. Bright-field imaging showed the presence of pronuclei at the vertical arrow (the scale bar represents 50  $\mu\text{m}$ ). Inset: in eggs in which the  $\text{Ca}^{2+}$  oscillations were above 600 nM, even the last  $\text{Ca}^{2+}$  spike was associated with cyclin destruction (diagonal arrow).

19. Kawahara, H., and Yokosawa, H. (1994). Intracellular calcium mobilization regulates the activity of the 26S proteasome during the metaphase-anaphase transition in the ascidian meiotic cell cycle. *Dev. Biol.* 166, 623–633.
20. Nakajima, T., Morita, K., Tsunoda, H., Imajoh-Ohmi, S., Tanaka, H., Yasuda, H., and Oda, K. (1998). Stabilization of p53 by adenovirus E1A occurs through its amino-terminal region by modification of the ubiquitin-proteasome pathway. *J. Biol. Chem.* 273, 20036–20045.
21. Hanson, P.J., Meyer, T., Stryer, L., and Schulman, H. (1994). Dual role of calmodulin in autophosphorylation of multifunctional CaM kinase may underlie decoding of calcium signals. *Neuron* 12, 943–956.
22. De Koninck, P., and Schulman, H. (1998). Sensitivity of CaM kinase II to the frequency of  $\text{Ca}^{2+}$  oscillations. *Science* 279, 227–230.
23. Miyazaki, S., Yuzaki, M., Nakada, K., Shirakawa, H., Nakanishi, S., Nakade, S., and Mikoshiba, K. (1992). Block of  $\text{Ca}^{2+}$  wave and  $\text{Ca}^{2+}$  oscillation by the antibody to the inositol 1,4,5-trisphosphate receptor in fertilized hamster eggs. *Science* 257, 251–255.
24. Kurasawa, S., Schultz, R.M., and Kopf, G.S. (1989). Egg-induced modifications of the zona pellucida of mouse eggs: effects of microinjected inositol 1,4,5-trisphosphate. *Dev. Biol.* 133, 295–304.
25. Deguchi, R., Shirakawa, H., Oda, S., Mohri, T., and Miyazaki, S. (2000). Spatiotemporal analysis of  $\text{Ca}^{2+}$  waves in relation to sperm entry site and animal-vegetal axis during  $\text{Ca}^{2+}$  oscillations in fertilized mouse eggs. *Dev. Biol.* 218, 299–313.
26. Yanagimachi, R. (1994). Mammalian fertilization. In *The Physiology of Reproduction*, Second Edition, E. Knobil and J.D. Neill, eds. (New York: Raven Press), pp. 189–317.
27. King, R., Deshaies, R.J., Peters, J., and Kirschner, M. (1996). How proteolysis drives the cell cycle. *Science* 274, 1652–1659.
28. Bastians, H., Topper, L.M., Gorbisky, G.L., and Ruderman, J.V. (1999). Cell cycle-regulated proteolysis of mitotic target proteins. *Mol. Biol. Cell* 10, 3927–3941.
29. Levasseur, M., and McDougall, A. (2000). Sperm-induced calcium oscillations at fertilisation in ascidians are controlled by cyclin B1-dependent kinase activity. *Development* 127, 631–641.
30. Jones, K.T., Soeller, C., and Cannell, M.B. (1998). The passage of  $\text{Ca}^{2+}$  and fluorescent markers between the sperm and egg after fusion in the mouse. *Development* 125, 4627–4635.
31. Hyslop, L.A., Carroll, M., Nixon, V.L., McDougall, A., and Jones, K.T. (2001). Simultaneous measurement of intracellular nitric oxide and free calcium levels in chordate eggs demonstrates that nitric oxide has no role at fertilization. *Dev. Biol.* 234, 216–230.
32. Tukey, J.W. (1977). *Exploratory Data Analysis*, First Edition (Reading: Addison-Wesley).
33. Jones, K.T., Carroll, J., and Whittingham, D.G. (1995). Ionomycin, thapsigargin, ryanodine, and sperm induced  $\text{Ca}^{2+}$  release increase during meiotic maturation of mouse oocytes. *J. Biol. Chem.* 270, 6671–6677.